

# Density mismatch in thin diblock copolymer films

S. Martins<sup>1</sup>, W.A.M. Morgado<sup>1</sup>, M.S.O. Massunaga<sup>2</sup> and M. Bahiana<sup>1</sup>

<sup>1</sup>*Instituto de Física, UFRJ, Caixa Postal 68528, Rio de Janeiro, RJ, Brazil, 21945-970*

<sup>2</sup>*Laboratório de Ciências Físicas, Universidade Estadual do Norte Fluminense,  
Av. Alberto Lamego 2000, Campos dos Goytacazes, RJ, Brazil, 28015-620*

(August 5, 2018)

Thin films of diblock copolymer subject to gravitational field are simulated by means of a cell dynamical system model. The difference in density of the two sides of the molecule and the presence of the field causes the formation of lamellar patterns with orientation parallel to the confining walls even when they are neutral. The concentration profile of those films is analyzed in the weak segregation regime and a functional form for the profile is proposed.

61.41.+e,64.60.Cn,64.75.+g

## I. INTRODUCTION

Recently, there has been a great deal of interest in problems involving periodic patterns in the tens of nanometers scale, for example, light conduction by photonic crystals [1], Josephson junctions arrays formed by granular superconducting materials [2], and lithographic masks for special design chips [3] among others.

In special, nanolithography has brought considerable attention to thin films of microphase separated diblock copolymers (DBCP) as they naturally self organize in periodic structures on that length scale [3–5].

The basic technique for the fabrication of those templates is the creation of a well-ordered DBCP film between two flat surfaces and then the transfer of the microdomains to a substrate where one of the components is removed leaving behind an ordered array of stripes or dots in either low or high relief. The desirable ordering, in this case, is one that creates a pattern on the substrate; for example, for even DBCP molecules one must have lamellae perpendicular to the hard boundaries.

For that matter it is important to understand the pattern formation in confined films of DBCP since it involves problems not present in bulk systems. This issue has been addressed both theoretically [6–9] and experimentally [10–12] and the basic conclusions are that, when the confining walls are neutral, the equilibrium pattern corresponds to lamellae perpendicular to the walls and, when the substrate prefers one kind of monomer, the pattern may consist of lamellae parallel or perpendicular to the walls, depending on the relation between the film thickness and the bulk lamellar width. The later effect appears because the finiteness of the system brings about frustration and one has to take into account the amount of compression or stretching of the molecules in order to accommodate a certain number of lamellae between the two rigid walls.

One important issue that has not been emphasized in the above studies is the possibility of density mismatch between the two parts of the molecules. At the bottom wall, as the denser part of the molecule sinks, lamellae parallel to the walls will form, even if the walls are neutral [13,14]. Being a bulk effect, the interaction with the gravitational field is capable of dramatically changing the microphase separation, even for infinite systems, as the lamellae tend to be aligned with the field far from the boundaries [13]. In finite systems, the lamellae perpendicular to the field present more diffuse interfaces and the gravitational field may completely destroy the microphase separation [14]. In the present work we consider this problem on two-dimensional films of even DBCP molecules as we analyze the effects of the degree of polymerization and film thickness on frustration by means of a cell dynamical system(CDS) model. We simulate films both in the weak and strong segregation regimes ((WSR)and (SSR)). For the WSR we empirically find the one-dimensional concentration profile and study the distortion of each layer within the lamellae.

In Sec. II, we define the model and outline the numerical scheme. Results for neutral and interacting walls in the presence and absence of the gravitational field are discussed in Sec. III. The effects of frustration are analyzed as they affect not only the size and number of lamellae, but also their internal structure. In section V, the main conclusions are summarized.

## II. COMPUTATIONAL MODEL

Block copolymers are linear-chain molecules consisting of two subchains  $A$  and  $B$  grafted covalently to each other. Below some critical temperature  $T_c$  these two blocks tend to separate, but due to the covalent bond, they can segregate

at best locally to form periodic structures [4]. Here we consider only the case of even molecules corresponding to lamellar equilibrium patterns. CDS models have been successfully used in several problems of phase separation dynamics due to their computational efficiency and versatility [15–20], so we prefer that method for the simulations. As usual, in this kind of description we assign a scalar variable  $\psi(n, t)$  to each lattice site corresponding to the coarse-grained order parameter in the  $n$ -th cell at time  $t$  (time here is defined as the number of iterations). This order parameter represents the difference  $\psi_A - \psi_B$ , where  $\psi_A(\psi_B)$  is the local number density of  $A(B)$ . The ingredients for the time evolution of  $\psi$  are: local dynamics dictated by a function with two symmetric hyperbolic attractive fixed points, diffusive coupling with neighbors, stabilization of the homogeneous solution and conservation of  $\psi$ . For the present problem, we also add the interaction with the gravitational field and with the confining walls. The conservation, when an external field is present, must be imposed by considering the Kawasaki exchange dynamics explicitly. The detailed explanation of this model is found in [21] for spinodal decomposition. With this, we come to final equation for a melt of even DBCP molecules:

$$\psi(n, t+1) = (1 - \epsilon)\psi(n, t) + \langle \langle C(n, j; \text{sgn}[I(n, t) - I(j, t)]) [I(n, t) - I(j, t)] \rangle \rangle, \quad (1)$$

where

$$I(n, t) \equiv \mathcal{A} \tanh(\psi(n, t)) - \psi(n, t) + D[\langle \langle \psi(n, t) \rangle \rangle - \psi(n, t)] + hn_z + V_s(n) \quad (2)$$

is essentially the chemical potential.  $\langle \langle \star \rangle \rangle$  is the isotropic space average of  $\star$ ,  $\mathcal{A}$  is a measure of the quench depth, and  $D$  is the diffusion coefficient. The parameter  $\epsilon > 0$  appears in this model to stabilize the solution  $\psi = 0$  in the bulk, for  $\epsilon = 0$  we have a model for spinodal decomposition, in which the domains can grow without bound. Scaling arguments have proved that  $\epsilon \sim N^{-2}$ , where  $N$  is the polymerization index [22].  $h$  is the gravitational field, which we assume is in the  $z$  direction, and  $n_z$  is the  $z$  component of  $n$ . For molecules with matched densities we just take  $h = 0$ . A possible interaction with the walls appears via the surface term  $V_s(n)$ .  $C$  is the collision coefficient given by:  $C(i, j; \alpha) = [\psi_c + \alpha\psi(j)][\psi_c - \alpha\psi(i)]/\psi_c^2$ , where  $\pm\psi_c$  are the fixed points of  $\mathcal{A} \tanh \psi - \psi$  for  $\mathcal{A} > 1$ . For all the simulations we used the values  $\mathcal{A} = 1.2$  and  $D = 0.5$ , and uniformly distributed random initial conditions. The gravitational field, when present, is parallel to the smaller dimension. The direction normal to the field will be called the  $x$  direction. We consider systems with periodic boundary conditions in the  $x$  direction and hard walls in the  $z$  direction, separated by a distance  $L_z$ . At the hard walls we impose no flux boundary conditions in the form:  $[I(z+1) - I(z)]_{\text{boundaries}} = 0$ .

### III. RESULTS

In order to understand the effect of confinement on the lamellae width, we must first determine its bulk value. For that matter, we ran simulations on  $512 \times 512$  lattices with periodic boundary conditions for different values of  $\epsilon$ , and  $h = 0$ . The resulting isotropically striped pattern was then Fourier transformed, and the bulk lamellar width  $W_b$  was measured in a standard way. Defining one lamella as *ABBA* we have:

$$W_b = \frac{2\pi}{\langle k \rangle_{eq}}, \quad (3)$$

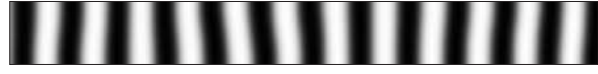
where

$$\langle k \rangle_{eq} = \frac{\int S(k, \infty) k dk}{\int S(k, \infty)}. \quad (4)$$

$S(k, \infty)$  is the circular average of the structure function  $S(\mathbf{k}, t) = |\psi(\mathbf{k}, t)|^2$ , calculated at large times, that is, when the value of  $\langle k \rangle$  approaches a constant value.

Just to make sure that the bulk lamellar width as measured above was not affected by the interface bending of the disordered pattern, we also measured  $W_b$  in  $32 \times 128$  systems with hard neutral walls and zero field, or matched densities. As expected the equilibrium configuration correspond to lamellae normal to the hard walls [9,12] as in Fig. 1(a).  $W_b$  was then measured using the one-dimensional structure function for each line and finally averaging along the  $z$  direction. The values of  $W_b$  found in both determinations agree, so we conclude that the excessive interface curving of the disordered pattern does not affect the lamellar width. Since the disordered patterns are easier to obtain, we will consider the lamellar width obtained from them as our bulk equilibrium value  $W_b$ .

The results below correspond to simulations with  $V_s = 0$  (neutral walls),  $h \neq 0$  (mismatched densities) and  $h = 0$  (matched densities), and  $V_s \neq 0$  (interacting walls) and  $h = 0$ . As will be seen, different patterns regarding the lamellae orientation appear: lamellae normal or parallel to the hard walls and a mixture of both.



(a)  $h=0$ ;  $\epsilon = 0.004$ ;  $V_s = 0$



(b)  $h=0.01$ ;  $\epsilon = 0.0014$ ;  $V_s = 0$



(c)  $h=0.01$ ;  $\epsilon = 0.01$ ;  $V_s = 0$



(d)  $h=0$ ;  $\epsilon = 0.01$ ;  $V_s = 0.01$

FIG. 1. Equilibrium patterns for confined films with  $L_z = 21$  and  $L_x = 256$  (only the first 150 columns are shown). (a) Neutral walls, and matched densities. The lamellae are normal to the walls with the bulk periodicity. (b) Neutral walls and density mismatch,  $\epsilon$  in the SSR. 1.5 lamellae are accommodated parallel to the walls. (c) Neutral walls and density mismatch,  $\epsilon$  in the WSR. 2.5 lamellae are formed parallel to the walls. The lamellar width is 8.401, smaller than the bulk value of 9.422. (d) Interacting walls and matched densities,  $\epsilon$  in the WSR. The lamellae are also parallel to the walls but are more segregated than in (c).

### A. Neutral walls

We focus now on films with mismatched densities ( $h \neq 0$ ), confined by neutral walls ( $V_s = 0$ ). In this situation we observe patterns of lamellae parallel to the hard walls, or a mixture of wetting layers on the hard walls and lamellae normal to the walls in the center part of the film. First we analyze the case of lamellae parallel to the walls only. Due to the density difference of chains  $A$  and  $B$ , the denser part (say  $A$ ) will be at the bottom, and the less dense part (say  $B$ ), at the top. For a blend of two homopolymers  $A$  and  $B$ , the film would have the lower half filled with  $A$  and the upper one with  $B$ . The covalent bond between  $A$  and  $B$  parts hinders this complete separation and forces the alternation of  $A$ -rich and  $B$ -rich microregions that will then have thicker interfaces due to the interpenetration of domains [14]. In the extreme case, the existence of a density mismatch may completely destroy the segregation of  $A$  and  $B$ . The number of alternating lamellae will depend on both chain size,  $\epsilon$ , (Fig. 1) and the separation between

walls,  $L_z$ , (see Figure 2). Also, the equilibrium patterns will always have  $m + 1/2$  lamellae, where  $m=0,1,2,\dots$

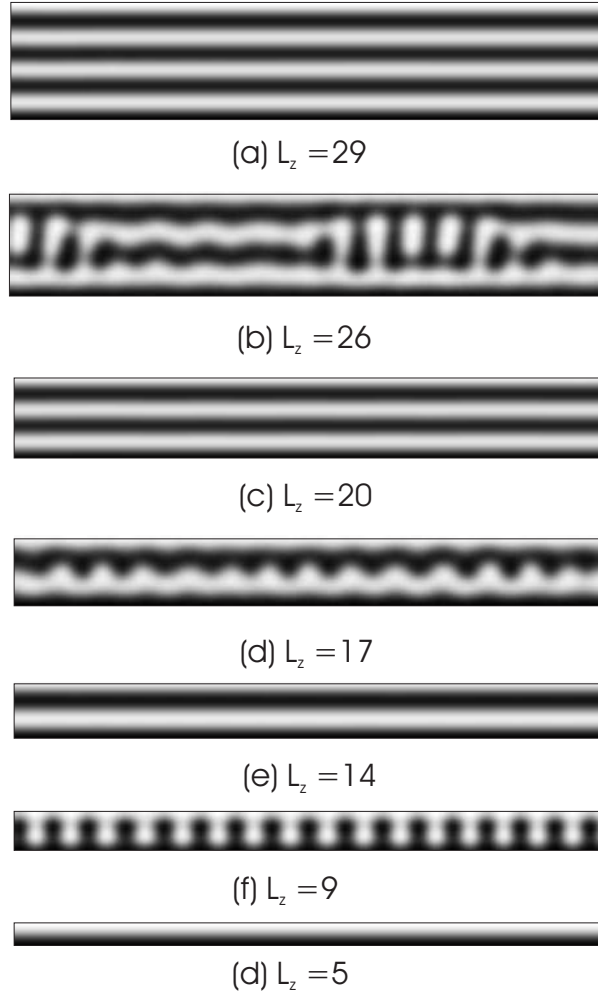


FIG. 2. Equilibrium patterns for films with  $h = 0.01$ ,  $\epsilon = 0.01$ (WSR) and variable width.  $L_x = 256$  but only the first 150 columns are shown. As the width  $L_z$  is decreased, the film goes discontinuously from  $m = 3$  to  $m = 0$  lamellar patterns. (b), (d) and (f) show transition patterns with mixed parallel and perpendicular lamellae.

As we vary  $L_z$  for a fixed  $\epsilon$  we clearly see the effects of frustration. Figure 2 shows the transitions from  $m = 0$ , to  $m = 1$ ,  $m = 2$  and  $m = 3$  patterns as  $L_z$  is changed from 5 to 29 for  $\epsilon = 0.01$  and  $h = 0.01$ . The transition patterns are frustrated and present lamellae normal to the walls in the central region. Since full lamellar patterns are essentially one dimensional, we define the average concentration profile,  $\langle \psi(n_z) \rangle_x$ , as the average over the  $x$  direction of the vertical variation of  $\psi$ . Figure 3 shows the behavior of  $\langle \psi(n_z) \rangle_x$ , for three different situations, for now we are interested in cases (a) and (b) only. Figure 3(a) corresponds to the profile for  $\epsilon = 0.01$ ,  $h = 0.01$ ,  $V_s = 0$  and  $L_z = 21$ . If we try to fit a sine function to that profile, we see that the fitting will miss only the wetting layers. From this we conclude that the system is in the WSR so that the inner layers can be described by just one Fourier component [23]. The wetting layers have an enhanced concentration due to gravitational field and the presence of the wall: the bottom and top  $AB$  layers are considerably stretched by the effect of buoyancy and do not experiment the penetration of other layers, resulting in an excess of  $A$  at the bottom and of  $B$  at the top.

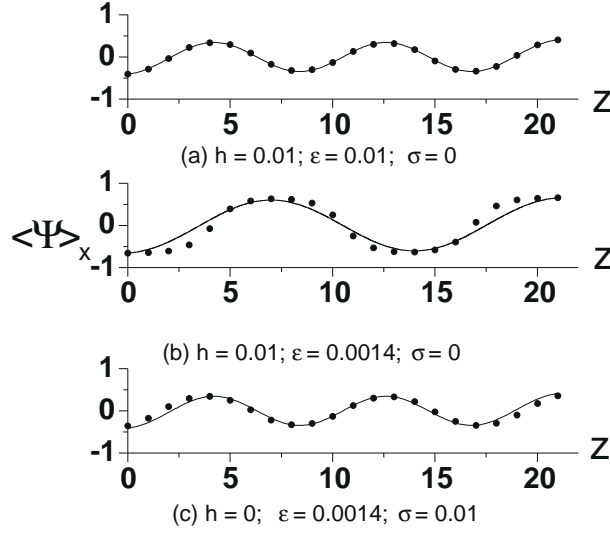


FIG. 3. Average concentration profiles for a film with  $L_z = 21$  and  $L_x = 256$ . The continuous line correspond to a fitting using Eq. (5) (a) Neutral walls, mismatched densities. The profile is well fitted by a sine function plus exponential enhancement at the hard walls. (b) Neutral walls, mismatched densities and molecules larger than in (a). From the fitting it is clear that more than one Fourier component must be considered, indicating that the film is already in the SSR; (c) Interacting walls ( $V_s(1) = -\sigma = -V_s(L_z)$ ) and matched densities. Although similar to the profile (a), we notice that Eq. (5) is not adequate to describe this concentration profile.

A correction for this effect led us to the tentative function

$$\psi(x) = (-1)^{m+1} \eta \sin qx + 2Ce^{-\beta L} \sinh 2\beta x \quad \text{for } -L/2 \leq x \leq L/2, \quad (5)$$

which fits very well the profile in Figure 3(a). For films in the WSR we found that the fitted value for  $q$  is indistinguishable from  $2\pi(m + 1/2)/L_z$ , so we define the average lamellar width  $W$ , directly from the fitting, as  $2\pi/q$ . As will be seen below, the interaction with the gravitational field causes a distortion within the lamellae regarding the width of the  $A$  and  $B$ -rich layers, but, if considered as a unit, all the lamellae have a width very close to the average value. The transitions between consecutive values of  $m$  as we vary  $L_z$  is shown in Figure 4. From this figure we see that discontinuous transitions occur from a pattern in which the lamellae are stretched, compared to its bulk state, to a compressed state with one more lamella, as  $L_z$  is increased. The regions between steps of fixed  $m$  correspond to transition patterns in which lamellae normal to the walls form in the center portion of the film.

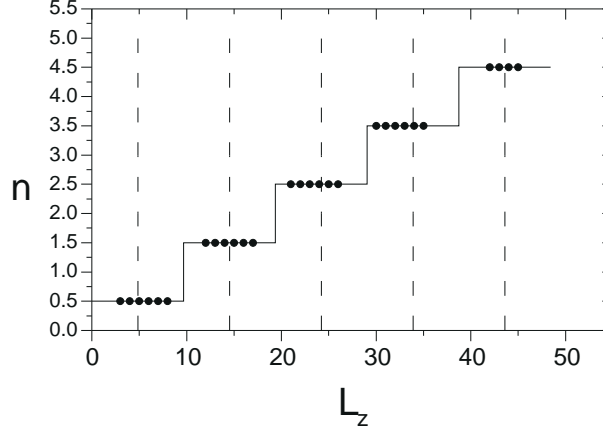


FIG. 4. Total number of lamellae,  $n$ , as a function of the film thickness  $L_z$  for a film with mismatched densities, confined by neutral walls. The solid points on the steps represent lamellar patterns with  $n$  lamellae parallel to the hard walls and between consecutive steps the film is in a mixed configuration with horizontal and vertical lamellae. The vertical dashed lines correspond to the film thickness adequate to accommodate the corresponding number of lamellae but with the bulk width  $W_b$ . We see that as the film width increases, discontinuous transitions between  $n$  stretched lamellae and  $n + 1$  compressed lamellae occur.

We can, alternatively, fix  $L_z$  and vary  $\epsilon$ , which corresponds to fixing the film width and varying the bulk lamellae width. For  $0.006 < \epsilon < 0.018$  we obtain patterns with  $m = 2$ , in the range  $0.004 < \epsilon < 0.006$  again we observe a transition pattern, and decreasing  $\epsilon$  further we find that a  $m = 1$  pattern appears. Figure 5 shows patterns with  $m=1$ ,  $m=2$  and in the transition region. The analysis of the transitions in this case is more complicated since for  $\epsilon < 0.004$  the system is no longer in the WSR as can be seen from the fitting of Eq. (5) in Fig. 3(b). It is clear that other Fourier components need to be included in this case.

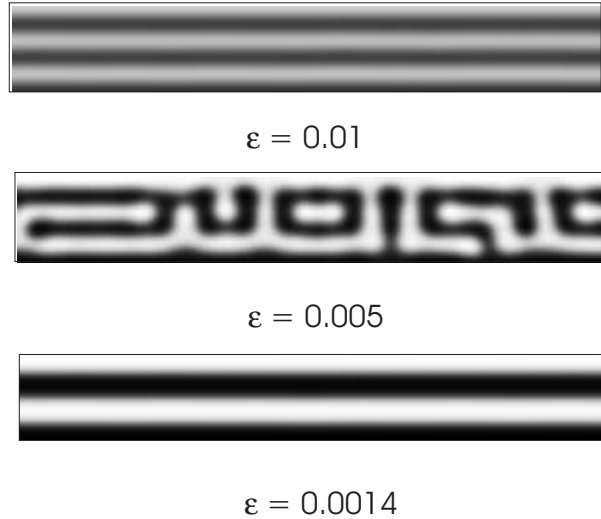


FIG. 5. Equilibrium patterns for confined films with  $L_z = 21$  and  $L_x = 256$  (only the first 150 columns are shown) three different values of  $\epsilon$ . As in the case of variable film width, the number of lamellae varies discontinuously and transition patterns with mixed orientation lamellae appear. For  $\epsilon = 0.01$  2.5 weakly segregated lamellae are formed, the concentration profile can be well fitted by Eq. 5.  $\epsilon = 0.005$  produces a transition pattern and  $\epsilon = 0.0014$ , a more segregated pattern with 1.5.

The accommodation of the lamellae distorts their widths non uniformly as may be easily checked from the plot of the width of each individual  $A$ -rich and  $B$ -rich layer. Figure 6 shows the behavior, as a function of  $\epsilon$ , of the widths of the first  $A$ -rich layer that wets the bottom wall ( $w_1$ ), the first  $B$ -rich layer connected to the bottom wetting layer ( $w_2$ ) and one quart of the central lamella ( $w_c = W/4$ ). For the sake of comparison, the variation of the bulk width,  $w_b = W_b/4$ , of  $A$ -rich (or  $B$ -rich) layers is also plotted. Although the variation is small compared to the bulk behavior, we see that  $w_2 < w_c < w_1$  consistently. This happens because there is a reduction in the number of  $A$  and  $B$  contacts in the first layer (for the lack of neighboring molecules from below) and an increase in the next one because the gravitational field shifts the  $A$  parts downwards. As we separate the regions where the lamellae are compressed and stretched as compared to the bulk, we notice two different situations. In the compressed region,  $w_1$  increases as  $N$  increases ( $\epsilon$  decreases), due to a compression of the internal layers caused by the greater stretching of the surface layers which produces an increase in the internal pressure (for  $L_z$  fixed). We expected the inverse effect to happen when  $N$  was reduced in the stretched region: the internal layers would shrink producing a tension that would stretch the surface (larger effect) and second layers (smaller effect). But, in fact, we observe a drastic reduction of the second layer acting as a tension center for surface and central layers (Fig. 6).

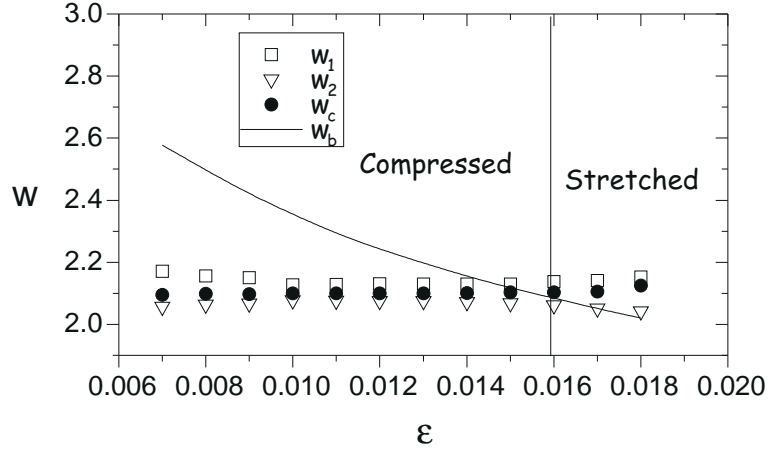


FIG. 6. Variation of  $A$ -rich and  $B$ -rich layers as a function of  $\epsilon$  for a films with 2.5 lamellae.  $w_1$ ,  $w_2$  are the widths of the lowest  $A$ -rich and  $B$ -rich layers,  $w_c$  is 1/4 of the central lamella and  $w_b$  is 1/4 of the bulk lamellar width. The vertical line indicates the separation between regions where the film is in compressed and stretched states.

It is clear that the above effects are meaningful only for thin films. The transition from this to the bulk behavior may be observed as we analyze  $w_1$ ,  $w_2$  and  $w_c$  as a function of the film thickness  $L_z$ . If the bulk behavior prevails,  $w_2 \approx w_1 \approx w_c \approx w_b \approx L_z/m$ . As we increase  $L_z$  and observe films with increasing number of lamellae, we find  $w_1 \rightarrow w_2 \rightarrow w_c \rightarrow w_b$ . On the other hand, the slope  $\alpha$  of each group of  $w$  values is proportional to  $m^{-0.8}$  instead of  $m^{-1}$ , which reflects the different behavior of each layer of DBCP under stretching or compressions.

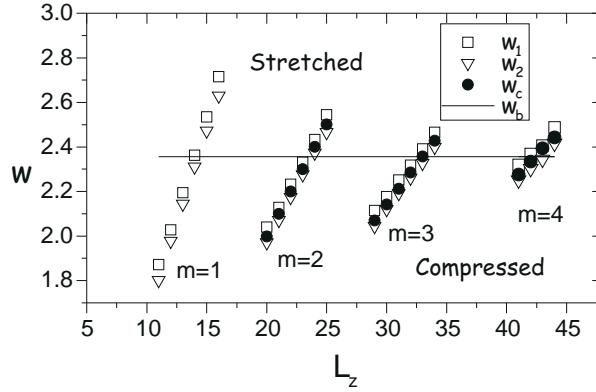


FIG. 7. Variation of  $A$ -rich and  $B$ -rich layers as a function of  $L_z$  for a films with  $\epsilon = 0.01$ . We use here the same notation of Fig. 6. Each group of points corresponds to lamellar patterns with  $(m + 1/2)$  lamellae. As  $L_z$ , and correspondingly  $m$ , increases, the film behaves more like a bulk sample in the sense that the distortion of lamellae is less significant. The slope  $\alpha$  of each group is proportional to  $m^{-0.8}$ , for larger values of  $L_z$  a crossover to the bulk behavior  $\alpha \propto m^{-1}$  is expected

## B. Interacting walls

The effect of surface fields in the formation of lamellar patterns has been extensively studied [6–12]. Our goal here is to compare the effect of the surface and bulk fields, so we consider only a film of DBCP molecules with matched densities confined by interacting walls in such a way that the bottom wall attracts the denser component and the top wall prefers the less dense component. As will be seen below, in many ways this choice of walls produces a pattern is similar to the one obtained with neutral walls and a density mismatch, but the two situations are, in fact, different.

The above interaction with walls may be simulated by choosing the surface interaction as:  $V_s = \sigma$  for  $z = 1$  and  $V_s = -\sigma$  for  $z = L_z$ . The equilibrium pattern obtained for  $\epsilon = 0.01$ ,  $L_z = 21$ ,  $h = 0$  and  $\sigma = 0.01$  is very similar to the one with the same values of  $\epsilon$  and  $L_z$ ,  $\sigma = 0$  and  $h = 0.01$ , as both present 2.5 lamellae parallel to the walls (see Fig.

1 (c) and (d), respectively). The first distinction appears in the segregation of domains: it is clear that the pattern in Fig. 1(c) is less segregated due to effect of interpenetration of domains driven by the gravitational field. As we try to fit the concentration profile with Eq. (5) we notice that the patterns with density mismatch and surface interaction are also a little different in the surface region, so we conclude that Eq. (5) is a good fit for the concentration profile of lamellar patterns with density mismatch and neutral walls only. A substantial difference appears for larger values of  $h$  and  $\sigma$ . Figure 8 shows patterns with the same value of  $\epsilon = 0.01$  and  $L_z = 21$  but one with surface field only and the other with density mismatch only. In this case, the lamellar structure still exists for  $\sigma = 0.04$  but here, for  $h = \sigma$  the lamellar structure is completely destroyed in the center of the film.



(a)  $\epsilon = 0.01$ ;  $h = 0$ ;  $V_s = 0.04$



(b)  $\epsilon = 0.01$ ;  $h = 0.04$ ;  $V_s = 0$

FIG. 8. A comparison between bulk and surface interactions. (a) Interacting walls and matched densities. Although the surface interaction is stronger than the one considered so far, the only noticeable difference is the segregation of the wetting lamellae. (b) Neutral walls and mismatched densities. Increasing the value of the bulk field  $h$  by the same amount as the surface field the observed pattern changes dramatically: instead of a lamellae pattern we observe a frustrated mixed orientation pattern.

#### IV. CONCLUSIONS

In this paper, we study the effects of surface and bulk (gravitational) fields coupled with hard wall restrictions on the lamellar pattern formation of diblock copolymer systems. We find that the two are the predominant factors to determine the final equilibrium pattern: lamellae tend to form normal to the field and their number is determined by the ability of the system to resolve the frustration caused by the confinement. Unresolved patterns present a mixture of wetting lamellae normal to the field and lamellae parallel to the field in the central part of the film. The gravitational field also distorts the periodicity of the lamellar pattern. The bottom  $A$  layer is larger than it would be if placed in the central part of the film. On the other hand, the next  $B$  layer is narrower, in such a way that the first lamella, defined as the sequence  $ABBA$ , has a width very close to the central lamellae.

We obtained a good fit for the average concentration profile in the WSR by using a trial function which consists of the superposition of a sinusoidal function, characteristic of the WSR, and exponential functions for the enhanced concentration of the wetting layers.

#### ACKNOWLEDGMENTS

This work was partially supported by CNPq (Brazil) and Faperj (Rio de Janeiro).

- 
- [1] B. G. Levi, *Physics Today*, **17**, January 1997. J.D. Joannopoulos, R.B. Meade, J.N. Winn, *Photonic Crystals*, Princeton U. P., New York, 1995. J.D. Joannopoulos, P.R. Villeneuve, S. Fan, *Nature* **386**, 143 (1997).
  - [2] C. Lobb, *Physica B* **152**, 1 (1988). H.S.J. van der Zant *et al.*, *Phys. Rev. B*, **47**, 295 (1993).
  - [3] M. Park *et al.*, *Science* **276**, 1401 (1997).
  - [4] F.S. Bates and G.H. Fredrickson, *Phys. Today* **52**, 2 (1999).



- [5] Z.-R. Chen *et al.*, Science **277**, 1248 (1997).
- [6] M. S. Turner, Phys. Rev. Lett. **69**, 1788 (1992).
- [7] M. Kikuchi and K. Binder, Europhys. Lett. **21**, 427 (1993).
- [8] G. Brown and A. Chakrabarti, J. Chem. Phys. **102**, 1440 (1995).
- [9] G. T. Pickett and A. C. Balazs, Macromolecules **30**, 3097 (1997).
- [10] A. Menelle, T. P. Russell, and S. Anastasiadis, Phys. Rev. Lett. **68**, 67 (1992).
- [11] P. Lambooy *et al.*, Phys. Rev. Lett. **72**, 2899 (1994).
- [12] G. Kellogg *et al.*, Phys. Rev. Lett. **76**, 2503 (1996).
- [13] M. Bahiana, Physica A **257**, 307 (1998).
- [14] M. Bahiana and W.A.M. Morgado, Phys. Rev. E **58**, 4027 (1998).
- [15] Y. Oono and S. Puri, Phys. Rev. Lett. **58**, 863 (1987).
- [16] Y. Enomoto and K. Kawasaki, Mod. Phys. Lett. B **3**, 605 (1989).
- [17] A. Chakrabarti and J. D. Gunton, Phys. Rev. B **37**, 3798 (1988).
- [18] M. Bahiana and Y. Oono, Phys. Rev. A **41**, 6763 (1990).
- [19] M. Mondello and N. Goldenfeld, Phys. Rev. A **42**, 5865 (1990).
- [20] A. Shinozaki and Y. Oono, Phys. Rev. Lett. **66**, 173 (1991).
- [21] K. Kitahara, Y. Oono, and D. Jasnow, Mod. Phys. Lett. B **2**, 765 (1988).
- [22] Y. Oono and M. Bahiana, Phys. Rev. Lett. **61**, 1109 (1988).
- [23] L. Leibler, Macromolecules **13**, 1602 (1980).